ARCHIVES
of
FOUNDRY ENGINEERING

ISSN (2299-2944)
Volume 2026
Issue 2/2026

155 – 164

19/2

10.24425/afe.2026.158002

Published quarterly as the organ of the Foundry Commission of the Polish Academy of Sciences

Evaluation of Mechanical Properties of GTAW Hardfacing Intended for the Repair of Permanent Foundry Mold Components

R. Koňár *, M. Mičian
Department of Technological Engineering, Faculty of Mechanical Engineering, University of Zilina,
Univerzitna 8215/1, 010 26 Zilina, Slovakia
* Corresponding author: e-mail: radoslav.konar@fstroj.uniza.sk

Received 23.09.2025; accepted in revised form 05.03.2026; available online 14.07.2026

Abstract

The repair of permanent steel foundry moulds is a critical industrial challenge driven by the need to minimize production costs and extend tool life. Gas Tungsten Arc Welding (GTAW) hardfacing offers a cost-effective restoration method, yet the impact of substrate dilution on the functional performance of high-alloyed layers remains insufficiently quantified. This study presents a unique evaluation of the synergy between the dilution rate and the tribological stability of the iron-based UTP-A 696 alloy deposited on an S355JR substrate. Three experimental samples with varying numbers of layers were prepared to analyze the transition from the fusion line to the pure hardfacing zone. The level of dilution was determined using spectral analysis and energy-dispersive X-ray spectroscopy (EDX). The results, supported by statistical processing, demonstrate that while the first layer suffers from significant mixing, the subsequent layers achieve a stable martensitic microstructure with a high density of complex carbides. A key finding of this research is the identification of a critical threshold for maintaining a stable coefficient of friction (0.753), providing a practical methodology for optimizing repair cycles in foundry environments. The study concludes that achieving a balance between dilution and hardness (up to 64 HRC) is paramount for the operational integrity of renovated mold components.

Keywords: Hardfacing welds, GTAW welding, EDX analysis, Mechanical properties

1. Introduction

The current global economic environment is characterised by significantly rising costs. The high prices of steel, electricity, and human labour increase the demand for enhanced economic efficiency in industrial production. Consequently, repair and renovation technologies are being utilised more frequently for the restoration of machine components.

Depending on the extent of mould damage and the necessary amount of metal that is needed to restore the functional surfaces, the selection of the appropriate arc welding method – such as GMAW (Gas Metal Arc Welding), MMAW (Manual Metal Arc Welding), or GTAW (Gas Tungsten Arc Welding) – is determined [1, 2].

Arc welding methods represent a primary category of these repair technologies, being readily applicable in general engineering practice. A critical factor in any repair is the appropriate selection of the welding consumable material. This selection must consider both the chemical composition of the base material and the specific mechanical properties required from the repaired component.

Arc welding renovations represent a highly effective method for reducing economic costs by significantly extending the service life of steel casting moulds and other machine components [1].

During casting, foundry moulds are primarily stressed by the high thermal loading, which cyclically stresses the component and

leads to the formation of cracks and other defects (e.g., thermal fatigue). Additionally, mould wear is caused by the liquid metal contacting the mould cavity especially when casting aluminum alloys into steel molds (e.g., abrasion, erosion, cavitation, high-temperature corrosion). This wear is concentrated in the most exposed areas of the mould, specifically sharp edges, abrupt changes in the mould's cross-section, and regions where the liquid metal experiences turbulent flow. The service life of the molds is limited by the influence of a tribodegradation factors combination, as well as by their operating conditions [1, 5, 6].

Arc hardfacing technology is neither financially nor technologically demanding and can be easily implemented in typical production workshops. Arc hardfacing can be applied to a wide range of metal materials; it is predominantly utilised for steel. This method allows for the use of welding consumables whose chemical composition and mechanical properties either match the base material (substrate) or are specifically chosen to enhance the mechanical performance of the new surface. Hardfacing can produce surfaces that achieve high hardness, up to 64 HRC in steel, and offer excellent wear resistance while simultaneously maintaining strong weld integrity with the substrate [1-5].

Although all arc welding technologies are suitable for surface hardfacing, GTAW is often the least demanding in terms of implementation and typically does not require specialised welding equipment.

Extensive research has been conducted on the properties of hardfacing welds applied to steel molds. These studies primarily focus on comparing the mechanical characteristics of the hardfacing layer, including strength, hardness, wear resistance, and corrosion resistance [7-11]. Furthermore, several works [10-13, 15, 17] include detailed evaluations of the microstructure of the hardfacing weld, the heat-affected zone (HAZ), and the substrate itself. Authors such as Brezinova and Sutka, in their publications [2, 4-6], have specifically compared the influence of various additive materials and welding technologies on coating properties and assessed the role of microstructure on the resulting mechanical performance. Other studies [3, 5, 12, 16, 18] dealing with the evaluation of hard deposits focus predominantly on practical repair applications, often extending beyond foundry moulds. Critically, a comprehensive and systematic analysis concerning the influence of additive material dilution (mixing) with the substrate on the mechanical characteristics and microstructure of the final coatings remains notably absent in the published research literature.

The properties of hardfacing welds are evaluated using established, standardized methods. Hardness measurements are performed using the Rockwell and Vickers methods (HV, HRC), both along a traverse from the substrate into the weld bead, and directly on the surface of the hardfacing layer [7-11]. Image illustrating Vickers hardness measurement path on a weld cross-section. Wear resistance is assessed via common tribological tests, such as the "pin-on-flat" and "pin-on-disc" methods [10-13].

The uniqueness of this research lies in the comprehensive quantification of the synergy between the dilution rate and the tribological stability of the UTP-A 696 alloy, which is specifically designed for high-thermal stress environments. Unlike standard hardfacing studies that focus primarily on maximum hardness, this work identifies the critical threshold of mixing with the S355JR substrate that still maintains a stable friction coefficient. By analyzing the transition from a single-layer to a three-layer deposit, the study provides a precise methodology for optimizing repair cycles in the foundry industry, where balancing material consumption and surface integrity is paramount for extending the service life of permanent molds.

2. Objective and Methodology

The primary goal of this article is to analyze the influence of additive material dilution (mixing) with the steel substrate on the mechanical characteristics of a three-layer hardfacing weld deposited by GTAW. Manual GTAW welding technology was selected specifically for its simplicity, precise control of the heat input, and its superior operability, which allows for the deposition of short and narrow surface welds (down to 2 mm). Based on previous experimental work, the additive material chosen for GTAW hardfacing was UTP-A 696 (manufactured by Voestalpine Böhler Welding, Düsseldorf, Germany). It is noted that comparisons of various hardfacing welds, utilizing different arc welding technologies and different additive materials, have been extensively documented in prior publications [2, 4-6, 14].

To analyze the effect of filler material dilution with the substrate on the resulting performance hardfacing properties, three distinct hardfacing specimens were fabricated. Low-carbon weldable steel S355JR was chosen as the substrate (base material).

Low-carbon structural steel (S355JR) was selected as the substrate primarily due to its significantly different chemical composition compared to the filler material. This difference ensures pronounced variations in the properties of individual hardfacing layers due to dilution (mixing) with the base material. Three hardfacing layers were selected for the experiment because the third layer reliably achieves the required properties specified in the hardfacing material datasheet. When depositing this type of hardfacing material onto high-alloy tool steel (a typical industrial application), it can be anticipated that the desired properties would be achieved as early as the second deposited layer.

Hardfacing deposits were subsequently applied to the substrate in configurations of one, two, and three layers, respectively.

The procedure for evaluating the experimental hardfacing samples was as follows:

- non-destructive testing (visual and penetrant testing),
- spectral analysis of the chemical composition of individual layers and the substrate,
- hardness measurement,
- wear resistance measurement,
- energy-dispersive X-ray spectroscopy (EDX) analysis.

In comparison to the previously published work [6], the scientific paper offers a more comprehensive analysis and research, specifically focusing on the progression of hardness through individual hardfacing layers, detailed microstructure evaluation, and chemical composition analysis of the materials with respect to the dilution percentage.

3. Materials and methods

The primary goal of the experimental analysis is to assess the influence of additive material dilution with the steel substrate on

the mechanical properties of hardfacing welds. Specifically, the study focuses on quantifying the changes in hardness and wear resistance across single-layer, two-layer, and three-layer hardfacing deposits fabricated using the manual GTAW method. The evaluation of the mechanical properties of the overlays is supplemented by a microstructure analysis, focusing on the chemical composition of precipitates formed along the grain boundaries of the hardfacing's primary structure.

The base material (substrate) was a 20 mm thick plate of low-carbon structural steel S355JR (Material No. 1.0045, standard EN 10025-2, C max. 0.24 %, supplier: Vitkovice Steel a.s, Moravska Ostrava, Czech Republic). This low-carbon steel is commonly used for machine parts and welded steel structures. The specific material utilized exhibited a Carbon Equivalent Value (CEV) 0.422%, as documented in the inspection certificate.

The experimental samples were machined by milling and surface grinding to specific dimensions: 120 mm in length, 40 mm in width and 20 mm in thickness. The sample dimensions were deliberately chosen to enable all required experimental analyses (e.g., hardness, wear, and microstructure evaluation) to be performed on a single specimen. This approach ensured that the results obtained from different tests could be directly correlated and contextualized.

The detailed chemical composition of the S355JR steel, both according to the EN 10025-2 standard and the inspection certificate for the specific batch used, is presented in Table 1 [6].

Table 1.
Steel S355JR chemical composition according to standard EN 10025-2 and from the inspection certificate [1]

Steel S355JR chemical composition (wt.%)										
According to	C	Mn	Si	Cu	Nb	Al	S	P	Fe	C_{EV}
EN 10025-2	max. 0.240	max. 1.600	max. 0.550	-	-	-	max. 0.035	max. 0.035	balance	Max. 0.45%
Inspection certificate	0.170	1.490	0.013	0.020	0.020	0.035	0.003	0.011	balance	0.42%

The hardfacing layers were deposited using the GTAW process, designated as 141 according to EN ISO 4063. The UTP-A 696 filler metal (Mat. No. 1.3348) with a diameter of 1.6 mm was selected for the deposition. This specific material was chosen based on prior experimental comparisons of various filler metals, which identified UTP-A 696 as the most suitable for the current study. Preliminary analytical results, which served as the basis for selecting the GTAW process and the UTP-A 696 filler metal, have been previously published in [6].

UTP-A 696 is a molybdenum-alloyed high-speed steel (HSS) filler metal, primarily designed for GTAW. According to the EN 14700 standard, it is classified within the S Z Fe4 group. Its chemical system, characterized by a balanced combination of Mo, Cr, V, and W, facilitates the formation of a secondary hardening phase during the cooling process. The weld metal exhibits a predominantly martensitic microstructure interspersed with a high volume fraction of complex primary and secondary carbides. These carbides (mainly of the M_6C and MC types) are evenly distributed within the matrix, providing the necessary lattice strain and precipitation hardening effects to ensure high hardness and thermal stability.

The hardfacing deposits are distinguished by exceptional resistance to abrasive wear, even under conditions involving high compressive stresses and dynamic impact (shocks). A key feature of UTP-A 696 is its ability to maintain high hardness levels (typically 60–64 HRC) at elevated temperatures, making it suitable for tools and components subject to thermal cycling. Despite its high hardness, the tough martensitic matrix provides sufficient resistance against spalling and cracking under impact loading.

Due to its high alloy content, the deposited layers are primarily processed by grinding. However, if machining is required, the use of sintered carbide tools is mandatory. Common applications include the hardfacing of hot-work tools, cold-shear blades, and components in the woodworking and mining industries where maximum wear resistance is required.

The chemical composition of the UTP-A 696 filler metal is summarized in Table 2 [1].

Table 2.
The hardfacing additive material UTP-A 696 chemical composition according to the filler material standard

The additive material UTP-A 696 chemical composition (wt.%)							
C	Si	Mn	Cr	Mo	V	W	Fe
1.00	0.20	0.20	4.00	8.50	2.00	1.80	balance

The experimental hardfacing welds were produced using a MagicWave 2200 inverter welding power source (Fronius, Wels, Austria). A thoriated-free WL20 tungsten electrode (98% W, 2% La_2O_3) with a diameter of 2.4 mm was employed, utilizing an argon (Ar) shielding gas with a purity of 99.996% (purity 4.6). Welding was performed using direct current electrode negative (DCEN) polarity. All beads were deposited at a constant welding current of $I_Z = 120$ A. The average welding voltage, as recorded by the power source monitoring system, was $U_Z = 12.7$ V. To ensure structural integrity and meet the manufacturer's specifications for the UTP-A 696 filler metal, a constant interpass temperature of 200 °C was maintained throughout the process.

Three experimental specimens were prepared to investigate the impact of dilution between the filler metal and the substrate on the resulting mechanical properties. The first specimen consisted of a single-layer deposit comprising six individual weld beads. The second specimen was designed as a two-layer hardfacing, with each layer containing six beads, totalling 12 beads. The third specimen featured a three-layer configuration, consisting of 18 weld beads in total (six beads per layer). All weld beads were deposited to a

length of 100 mm. The schematic representation of the specimens, including the deposition sequence and bead arrangement, is illustrated in Figure 1 [1, 8].

Before the deposition of the first layer, the substrate surface was ground and cleaned to a metallic luster. The initial surface treatment of the substrate does not influence the final quality or properties of the cladding, as the GTAW process involves substrate penetration to a depth of at least 1 mm (Fig. 3). This fusion depth effectively eliminates any prior surface effects or mechanical history of the material. For subsequent layers, only mechanical cleaning of the surface was performed.

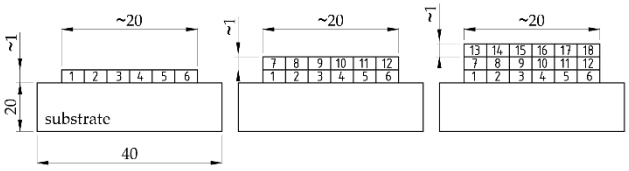

Fig. 1. Schematic representation of the deposition sequence for: a) one-layer, b) two-layer, and c) three-layer hardfacing specimens

The surface morphology of the as-welded GTAW hardfacings is presented in Figure 2.

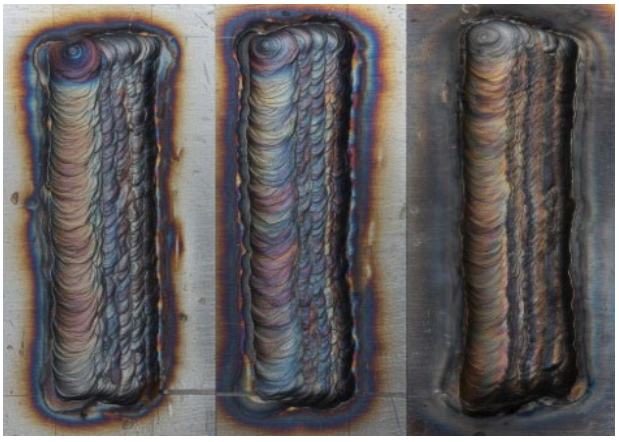

Fig. 2. Visual appearance and surface morphology of the GTAW hardfacing specimens: a) one-layer deposit, b) two-layer deposit, and c) three-layer deposit in the as-welded state

3. Experimental analysis and measurements

The experimental investigation was conducted according to the following sequence of steps:

- non-destructive testing (NDT): visual (Figure 2) and liquid penetrant testing,
- macrostructural analysis: characterization of the weld geometry and heat-affected zone (Figure 3),
- hardness testing: vickers hardness profiles across the hardfacing layers (Figure 4, Figure 5),
- chemical composition analysis: verification of alloying element distribution (Figure 6),
- wear resistance evaluation: tribological testing of the deposited surfaces (Figure 7),
- microstructural characterization: analysis using light microscopy (Figure 10),
- EDX analysis: elemental mapping and phase identification (Figure 14).

The experimental specimens were initially subjected to non-destructive testing (NDT). Visual (VT) and liquid penetrant (PT) inspections were conducted once the hardfacings had cooled to an ambient temperature. The primary objective of these inspections was to detect and evaluate potential surface defects and geometric deviations, such as cracks, lack of fusion, and porosity. Visual testing was performed in accordance with EN ISO 17637, while penetrant testing followed EN ISO 23277. No defects were detected during the NDT phase. The quality of the deposited layers was assessed against the most stringent requirements of EN ISO 5817, meeting quality level B. Consequently, the hardfacing surfaces were confirmed to be defect-free.

The second phase involved the evaluation of the macrostructure. Metallographic specimens were prepared by cross-sectioning the welds in a direction perpendicular to the welding axis. The geometric parameters of the individual weld beads and hardfacing layers were measured using AutoCAD software. The resulting macrostructures, illustrating the penetration depth and layer arrangement, are presented in Figure 3.

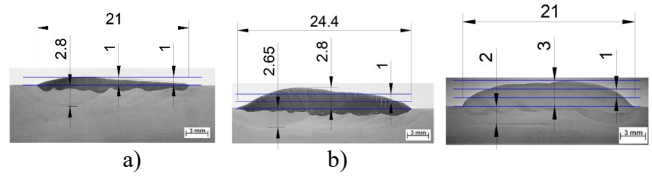

Fig. 3. Cross-sectional macrostructure of the GTAW hardfacing layers: a) one-layer, b) two-layer, and c) three-layer deposit

The surface of the hardfacing deposits was ground to a surface roughness of R_a = 0.8 μm to ensure precise and repeatable Rockwell hardness measurements. The grinding process was performed under continuous cooling with a cutting fluid to ensure minimal thermal influence on the material. This precaution prevented any localized tempering or microstructural changes that could lead to inaccuracies during hardness testing. Proper surface preparation is essential for Rockwell hardness testing, as surface irregularities can lead to inaccurate readings and potential damage to the diamond indenter. Inconsistent contact between the indenter and a rough surface often results in false depth measurements, thereby underestimating the actual hardness of the hardfacing layer.

Surface hardness represents a critical parameter for evaluating the quality of the deposited layers, as it directly correlates with the material's suitability for specific industrial applications involving high mechanical stress or abrasive wear.

Surface hardness was measured using an AQUASTYL RB-1E/AQ Rockwell hardness tester (Považská Bystrica, Slovakia). In addition to the final surfaces, the hardness of individual internal

layers in multi-layer deposits was evaluated. To access these internal layers, the specimens were precisely ground to the required depths, which were determined based on the macrostructural analysis (Figure 3). For each layer, a total of 12 measurements were performed, with the indentations distributed evenly across the prepared surface. The average hardness values, summarized in Table 3, were calculated from these 12 readings.

Table 3.
The average surface hardfacing hardness

Experimental sample	Layer	Average hardness [HRC]
One-layer	1st	60±1
Two-layer	1st	61±1
	2nd	63±1
Three-layer	1st	63±1
	2nd	63±1
	3rd	64±1

The Rockwell hardness measurement consistency was high, with the variance between the maximum and minimum values not exceeding 2 HRC.

A second series of hardness measurements was conducted to determine the hardness profile along a linear path extending from the hardfacing surface, through the heat-affected zone, and into the base material. These measurements were performed using the Vickers microhardness method (HV1) on cross-sectional specimens cut perpendicular to the welding axis. The measurement profile followed a vertical trajectory, starting at the deposit face and progressing through the fusion boundary to capture the metallurgical transitions. The specific orientation and locations of these measurement lines for each specimen are illustrated in Figure 4.

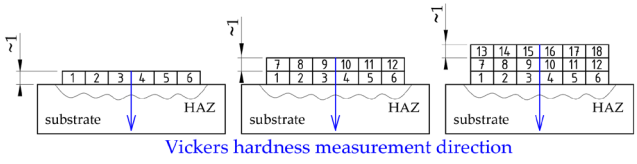

Fig. 4. Macrostructure of the single-layer GTAW hardfacing with a designated measurement line

To evaluate the hardness gradient from the hardfacing surface to the base material, the Vickers hardness testing method (HV1) was employed with a load of 9.807 N. The measurements were performed using an Innovatest 412D testing machine (Innovatest Europe BV, Maastricht, Netherlands) in compliance with the EN ISO 9015-1 standard. To ensure high resolution of the hardness profile, a constant distance of 0.25 mm was maintained between individual indentations. The resulting hardness distribution profiles for all specimens are presented in Figure 5.

The maximum hardness of 1015 HV1 was recorded in the three-layer hardfacing at a distance of 0.5 mm from the surface. In comparison, the single-layer deposit reached a peak hardness of only 850 HV1 at a distance 0.25 mm. This significant difference (approximately 20%) is attributed to the reduced dilution rate in multi-layer welding, where subsequent layers preserve the chemical composition and microstructural integrity of the hardfacing alloy.

The dilution of the filler metal with the substrate was evaluated by comparing the chemical composition of the hardfacing with the values specified in the technical data sheet for the UTP-A 696 filler material.

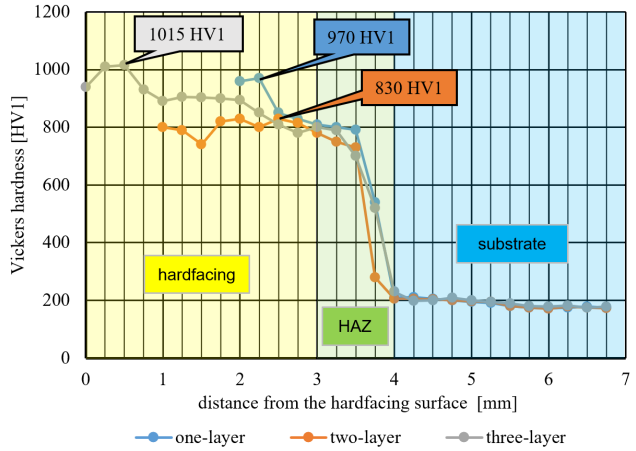

Fig. 5. Vickers HV1 hardness profile with maximum hardness values of individual hardfacings

Chemical analysis was performed on the same ground surfaces previously prepared for Rockwell hardness testing. Chemical analysis was performed using a Q2 ION BRUKER spark optical emission spectrometer. This instrument is capable of detecting key alloying elements, such as carbon (C), chromium (Cr), nickel (Ni), molybdene (Mo) and manganese (Mn), with a high degree of repeatability. The limits of detection (LOD) for common alloying elements range from 0.001% to 0.01%. For major elements with concentrations exceeding 1% (e.g., Cr in the hardfacing), the relative standard deviation (RSD) is typically below 1%, ensuring high measurement precision. For trace elements (with content below 0.1%), the RSD generally ranges between 2% and 5%.

The layer designated as 0th' in Table 4 represents the surface ground down to the plane of the base material. The chemical composition measured on the surface of the individual hardfacing layers is summarized in Table 4.

The dilution of individual layers with the substrate (or with the preceding layer) was determined based on the areas identified during the macrostructural analysis. Mathematically, this calculation can be expressed as follows:

$$D = \frac{A_{sub}}{A_{re}+A_{sub}} . 100\%, \quad (1)$$

D [%] - diluton (mixing) of the layers,
A_{sub} $[m^2]$ - represents the area of the melted substrate,
A_{re} $[m^2]$ - represents the reinforcement area.

Table 4.
Chemical composition of hardfacing layers [wt.%]

Sample	Dilution D [%]	Layer	C	W	V	Mn	Si	Cr	Mo	Ni	Cu	Fe
One-layer	19%	0th	0.38	-	0.89	0.83	0.29	1.83	3.07	0.06	0.11	92.20
	25%	1st	0.42	-	1.09	0.86	0.26	2.05	3.57	0.05	0.11	91.40
Two-layer	26%	1st	0.75	-	1.08	0.50	0.32	3.31	5.71	0.08	0.16	86.90
	31%	2nd	0.78	-	1.07	0.45	0.34	3.45	6.30	0.06	0.15	87.90
Three-layer	24%	1st	0.57	-	1.08	0.55	0.40	2.96	4.93	0.09	0.16	88.40
	28%	2nd	0.80	-	1.08	0.40	0.30	3.50	6.50	0.07	0.15	85.40
	35%	3rd	0.87	0.89	1.56	0.40	0.30	3.30	7.40	0.12	0.17	83.20

The distribution of chemical elements across the individual layers of the three-layer hardfacing is illustrated in Figure 6. The graph demonstrates the variation in elemental content resulting from the dilution of the filler metal with the base material. The chemical composition aligns most closely with the nominal values of the hardfacing alloy only within the third-layer of the deposit. Minor discrepancies in the elemental content may be attributed to the burnout of alloying elements within the weld pool during the welding process.

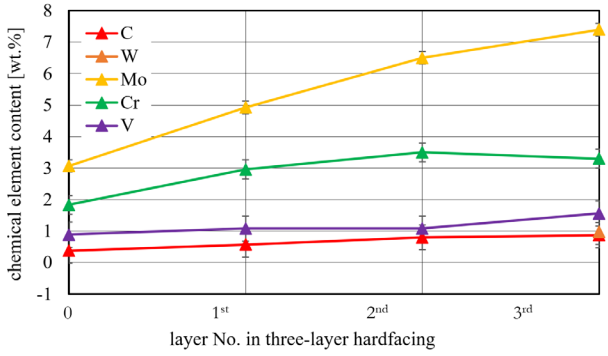

Fig. 6. The chemical element content in the individual layers of the three-layer hardfacing

This stabilization of the chemical composition in the third layer directly correlates with the maximum hardness values exceeding 1000 HV1 observed in the previous measurements.

Tribological properties were evaluated using a linear reciprocating wear test (ball-on-flat geometry). A hardened 100Cr6 steel ball with a diameter of 3 mm was used as the counter-body. The test was conducted with a sinusoidal velocity profile over a total sliding distance of 50 mm with a velocity of v = 0.017 m.s^{-1}. To ensure consistency and eliminate dynamic shocks during direction changes in the reciprocating motion, the normal load was maintained at a constant 10 N using an automated closed-loop force control system. Before the measurement, the surface of the hardfacing layers was ground to a roughness of Ra = 3.6 µm using intensive fluid cooling to prevent any thermal influence (grinding burn) on the surface hardness.

The test was conducted under dry sliding conditions (without lubrication) at an ambient temperature of 20°C. Total test duration of 5000 s. The resulting wear tracks on the sample surfaces after the tribological testing are illustrated in Figure 7.

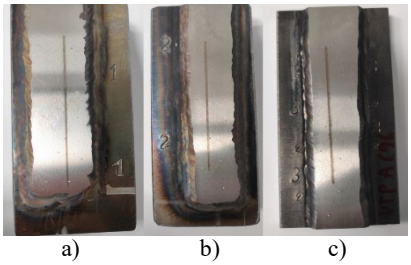

Fig. 7. Experimental hardfacing after tribological testing: a) one-layer; b) two-layer, c) three-layer

The total sliding distance covered by the pin was approximately 85 m. A precise determination of the distance was hindered by the sinusoidal velocity profile, which involved continuous acceleration and deceleration throughout each stroke.

The friction coefficient was determined through tribological testing for all hardfacing samples. The measured values were plotted as a function of time to evaluate the stability of the friction process. The resulting time-dependent friction coefficient curves for the single-layer, double-layer, and triple-layer hardfacings are illustrated in Figure 8. These curves provide insight into the running-in behavior and the subsequent steady-state friction regime of the deposited layers under dry sliding conditions.

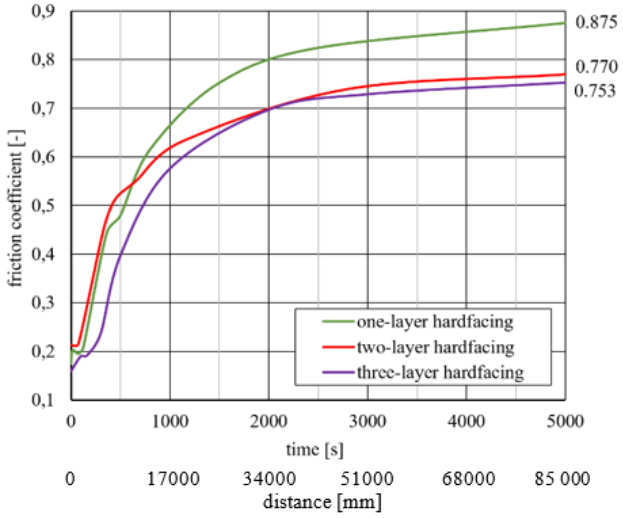

Fig. 8. The friction surface coefficient for one-layer, two-layer, and three-layer hardfacing

The friction coefficient for the one-layer coating rises sharply at the beginning of the test, reaching 0.670 at 1000 s. By the end of the 5000 s test period, the coefficient increased to a maximum value of 0.875.

Similarly, the friction coefficient for the two-layer hardfacing surface increases rapidly during the first 1000 s, reaching a value of 0.625. At the conclusion of the test (5000 s), the friction coefficient reached 0.770.

For the three-layer hardfacing, the coefficient of friction reached 0.576 at the 1000 s mark. The progression within this time interval followed a similar trend to that of the two-layer deposit. Notably, this sample exhibited the lowest friction coefficient at the end of the test, specifically 0.753.

The friction coefficient curves for the two and three-layer surfaces are very similar, which can be attributed to their comparable chemical compositions. Dilution of the filler metal with the base material is minimized in the third layer of the three-layer deposit. These results suggest that even a two-layer application is sufficient to achieve tribological properties close to those of the nominal hardfacing material.

Additionally, friction coefficients were measured across the individual layers of the three-layer hardfacing. These measurements were performed on the same surfaces used for HRC hardness testing and chemical composition analysis, ensuring a direct correlation between the data sets. A comprehensive comparison of the friction coefficients for the one-layer, two-layer, and individual layers of the three-layer hardfacing is presented in Figure 9.

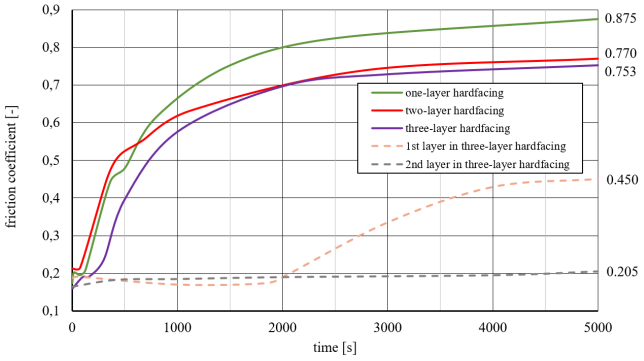

Fig. 9. The surface friction coefficient for one-layer hardfacing and three-layer hardfacing ground to the first layer

Significant differences in the friction coefficient values are evident from the trends presented in Figure 9. The analysis of individual layers within the three-layer hardfacing yielded particularly compelling results. While the final third layer reached a friction coefficient of 0.753 by the end of the test, the 1st layer – measured after grinding down the upper layers – exhibited a value of 0.450. This represents a notable 40% decrease in the friction coefficient compared to the top surface.

The superior tribological performance was observed in the 2nd layer of the three-layer deposit, which achieved the lowest friction coefficient of 0.205. This represents a significant 73% reduction compared to the top surface (third layer). The primary factor contributing to this substantial improvement is the in-situ annealing (self-tempering) of the underlying layers caused by the thermal cycles of subsequent welding passes. This thermal effect promotes the precipitation of complex secondary carbides within the martensitic matrix, which significantly enhances wear resistance and stabilizes the friction process by providing a higher density of hard particles compared to the as-welded state of the third layer. The observed reduction in friction coefficient in the second layer is linked to the secondary hardening effect, characterized by the precipitation of fine $M_{23}C_6$, M_2C and MC type carbides (where is primarily V, W or Mo), which refine the microstructure and increase the resistance to adhesive wear casting.

The friction coefficient was evaluated in its steady-state phase after the initial run-in period. Although the total sliding distance was 85 m (time of 5000 s and average velocity of 0.017 $m.s^{-1}$), this interval provided sufficient data to characterize the interface stability between the 100Cr6 ball and the UTP-A 696 hardfacing. The observed fluctuations in friction coefficient were minimal, confirming that the ground surface (Ra 3.6 µm) provided a stable contact area without premature adhesive failure. While Archard's unit wear rate (k) and cross-sectional wear profiles offer valuable data for long-term wear prediction, this study prioritizes the immediate frictional response, which is a primary indicator of mold release performance and early-stage tool degradation in foundry environments.

Microstructural analysis was conducted following the hardness and wear resistance measurements to correlate the mechanical properties with the material's state. The substrate exhibited characteristic structures typical for S355JR steel subjected to the welding thermal cycle. The base material displayed a typical banded ferritic-pearlitic microstructure. In contrast, the heat-affected zone was characterized by a needle-like (acicular) structure, resulting from the rapid heating into the austenitic region followed by subsequent transformation during cooling. The microstructural evolution across the individual regions of the substrate is illustrated in Figure 10.

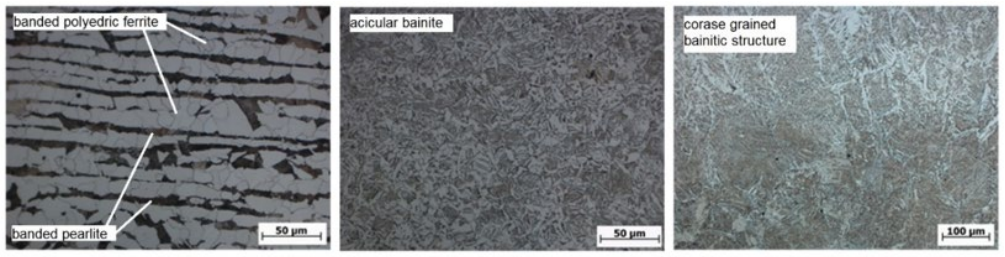

Fig. 10. Base material S355 JR microstructure: a) base material, b) heat-affected zone, c) grain growth HAZ

The microstructure of the hardfacing was further investigated, focusing on the third bead (the top surface) of the three-layer deposit. A Tescan SEM Mira3 scanning electron microscope (Tescan, Brno, Czech Republic) equipped with a BSE detector was employed for this analysis. The investigation revealed a characteristic dendritic structure of the deposit, featuring a significant distribution of precipitated complex carbides. These carbides are predominantly localized along the interdendritic boundaries. The representative microstructure of the hardfacing weld at various magnifications is illustrated in Figure 11.

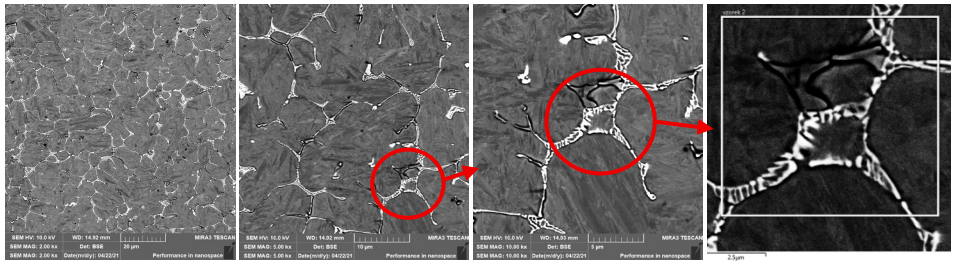

a) b) c) d)

Fig. 11. The microstructure of the top layer (third bead) of the three-layer hardfacing: a) 2000x, b) 5000x, c) 10000x, d) 20000x

The observed dendritic morphology is a direct consequence of the solidification physics inherent to the GTAW process. The high temperature gradient (G) at the fusion line, combined with the rapid growth rate (R) of the crystals during cooling, leads to constitutional supercooling. This environment suppresses a planar solidification front in favor of a dendritic one. The primary and secondary dendrite arms develop in the direction of the heat flow, while alloying elements such as W, V, and Cr are partitioned into the interdendritic spaces, where they subsequently form complex carbides during the final stages of solidification.

Chemical analysis was performed using the same SEM device equipped with an energy-dispersive X-ray spectroscopy (EDX) system. The instrument is capable of determining the elemental weight content with an accuracy of ±0.1 wt.%. The samples for EDS analysis were polished to a finish using 1µm particles and analyzed in an unetched state. The spatial distribution of alloying elements within the hardfacing microstructure is visualized using a color-coded mapping scale. Figure 13 displays the complex chemical composition of the deposit, providing an overview of the elemental distribution. The specific mapping for individual elements – Tungsten (W), Silicon (Si), Iron (Fe), Molybdenum (Mo), and Chromium (Cr) – is presented, highlighting the segregation of heavy alloying elements into the interdendritic regions.

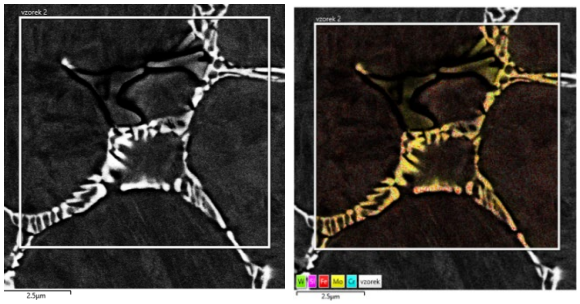

Fig. 12. Complex display of chemical elements in the third bead of the three-layer hardfacing

The analysis reveals a distinct correlation between the microstructural phases and the distribution of alloying elements. The color-coded map confirms that heavy carbide-forming elements, specifically Tungsten (W), Molybdenum (Mo), and Chromium (Cr), are heavily concentrated in the interdendritic bright phases. The overlapping of these signals (visible as yellowish-white regions in the composite map) indicates the formation of complex $M_{23}C6$, M_6C type carbides. In contrast, the darker regions (martensitic matrix) show a predominant concentration of Iron (Fe), with a significantly lower presence of the aforementioned alloying elements.

Individual display of chemical elements at the measurement location is shown in Figure 13.

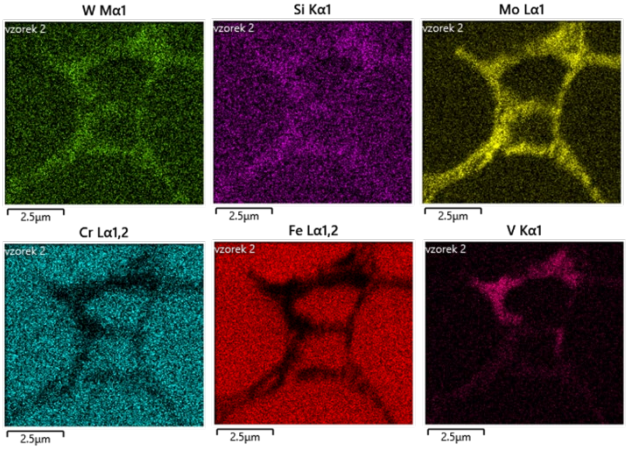

Fig. 13. Individual display of chemical elements in third bead of the three-layer hardfacing

The individual maps for Tungsten (W), Silicon (Si), Iron (Fe), Molybdenum (Mo), Chromium (Cr), and Vanadium (V) reveal the following:

- carbide-forming elements (W, Mo, Cr, V) – these elements show a clear concentration in the interdendritic regions. This segregation indicates the formation of complex carbides – specifically M_6C (rich in W and Mo), $M_{23}C_6$ (rich in Cr), and MC (rich in V),
- vanadium (V) – the V map shows specific enrichment zones, which are critical as the precipitation of fine secondary

vanadium carbides is the primary factor in reducing the friction coefficient,

- iron (Fe) – the Fe distribution acts as a negative of the carbide network, dominating the dendritic cores that form the martensitic matrix.
- silicon (Si) – this element is distributed more uniformly across the area, contributing to the overall stability of the matrix.

To supplement the elemental mapping, the local chemical composition was verified by point EDX analysis. Measurement sites were strategically selected at complex carbide locations to ascertain their stoichiometric tendencies. The quantitative results are illustrated in Figure 14.

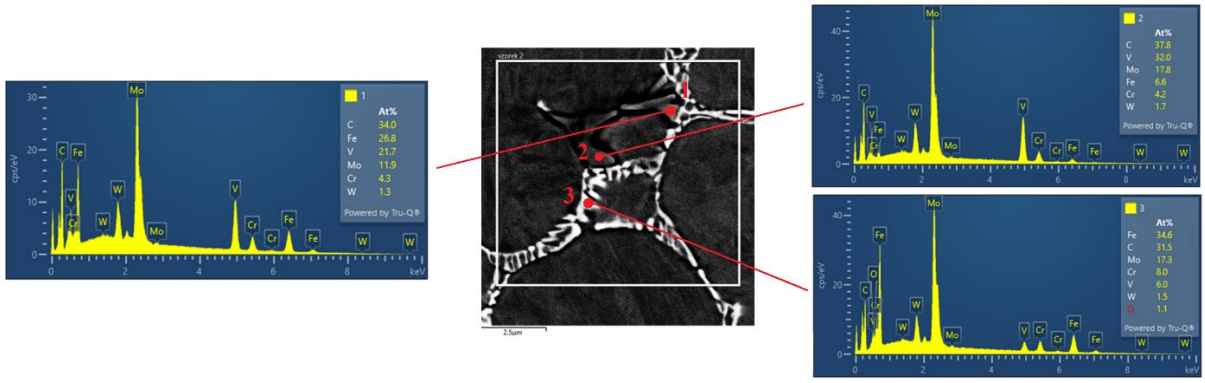

Fig. 14. EDX analysis of carbides in the third bead of the three-layer hardfacing

The EDX analysis of carbides within the third bead of the three-layer hardfacing confirmed the presence of complex phases with high concentrations of carbide-forming elements. In the third layer, dilution from the substrate is minimized, allowing for the full carbides precipitation. Point microanalysis (Figure 14) reveals that these carbides are significantly enriched with molybdenum and vanadium, directly contributing to the high hardness and thermal stability required for permanent foundry molds.

4. Conclusions

Based on the investigation of the structural composition, hardness measurements, wear resistance, and EDX microanalysis of the GTAW deposits, the following can be concluded:

1. Layer accumulation and dilution – the chemical composition closest to that of the filler metal was achieved only in the third layer of the hardfacing. Due to the minimal dilution with the substrate in this layer, a minimum of three layers is recommended to ensure the desired functional properties.
2. Tribological properties and grinding – the lowest friction coefficients were observed on the surface of the three-layer hardfacing. However, when comparing the internal layers (after grinding), the second layer exhibited the lowest friction coefficient. This is attributed to the secondary hardening effect of the second layer caused by the thermal cycles during the deposition of the third layer. Therefore, to achieve the optimal properties of the functional surface, it is advisable to remove the top layer by grinding.
3. Microstructure and carbide formation – the microstructure exhibits a typical dendritic casting morphology resulting from the rapid solidification of the melt. The dendritic morphology, with the primary dendrite axes oriented in the direction of the maximum cooling rate, is caused by heat dissipation into the substrate. In this case, the substrate acts as a heat sink, facilitating the formation of the desired hard microstructure. The hardfacing layer is characterized by a high-alloyed iron-based solid solution (martensitic matrix) with a significant presence of alloying elements like Cr, Mo, V, and W, which contribute to the formation of hard secondary phases, which are primarily responsible for the high hardness and enhanced wear resistance of the hardfacing.
4. Application potential – GTAW technology proved to be a suitable and robust method for producing high-quality hardfacings even in workshop conditions. Using the UTP-A 696 filler metal, it is possible to achieve excellent hardness and abrasion resistance without the necessity for additional heat treatment, while maintaining a minimal risk of cracks or fissures.
5. Future research directions should focus on the thermal fatigue resistance of the GTAW hardfacings under cyclic loading conditions typical for foundry operations. Additionally, the effect of preheating and interpass temperatures on residual stress distribution warrants detailed study. Future work could also employ electron backscatter diffraction (EBSD) to precisely characterize the crystallographic structure of the identified Mo-V carbides. Furthermore, future investigations should incorporate 3D profilometry of the worn surfaces to determine the specific wear rate according to Archard's wear law. This quantitative approach would enable a rigorous comparison of the hardfacing's wear resistance against other engineering materials. Finally, conducting high-temperature wear tests would provide a more comprehensive understanding of the tribological performance under real-world operating conditions.

Acknowledgements

The research leading was funded by the KEGA agency [grant number KEGA 018ŽU-4/2025]; VEGA agency [grant number VEGA 1/0181/26] and this work was supported by the Slovakia Program (Project code ITMS2021+: 401101C504).

References

[1] Moritzer, E. & Martin, Y. (2017). Experimental investigations on the fibre length degradation in injection moulds. In *AIP Conference Proceedings* (Vol. 1914(1), 140004). AIP Publishing. DOI: 10.1063/1.5016769.

[2] Brezinova, J., Dzupon, M., Vinas, J., Vojtko, M., Brezina, J., Vaskova, I. & Puchy, V. (2022). Possibilities of repairing functional surfaces of molds for injecting Al alloys using manual GTAW cladding. *Metals.* 12(11), 1781, 1-22. DOI: 10.3390/met12111781.

[3] Klobcar, D. & Tusek, J. (2008). Thermal stresses in aluminium alloy die casting dies. *Computational Materials Science.* 43(4), 1147-1154. DOI: 10.1016/j.commatsci. 2008.03.009.

[4] Brezinova, J., Draganovska, D., Guzanova, A., Balogh, P. & Vinas, J. (2016). Influence of the hardfacing welds structure on their wear resistance. *Metals.* 6(2), 36, 1-12. DOI: 10.3390/met6020036.

[5] Brezinová, J., Dzupon, M., Vinas, J., Guzanova, A., Puchy, V., Brezina, J., Draganovska, D. & Vojtko, M. (2020). Progresive CMT cladding for renovation of casting mold. *Acta Metallurgica Slovaca*. 26(3), 104-110. DOI: 10.36547/ams.26.3.565.

[6] Sutka, J. & Konar, R. (2023). The effect of mixing the additive material with the substrate during the renovation of the foundry mold by TIG welding hardfacing. *Manufacturing Technology*. 23(3), 341-347. DOI: 10.21062/mft.2023.033.

[7] Gülenç, B. & Kahraman, N. (2003). Wear behaviour of bulldozer rollers welded using a submerged arc welding process. *Materials & Design.* 24(7), 537-542. DOI: 10.1016/S0261-3069(03)00082-7.

[8] Beckowski, R. & Gucwa, M. (2016). Defects appearing in the surfacing layers of abrasion resistant. *Archives of Foundry Engineering.*16(4), 23-28. DOI: 10.1515/afe-2016-0077.

[9] Satwant, S., Raman, K., Panakj, G. & Harmeet, S. (2022). Analysis of wear and hardness during surface hardfacing of alloy steel by thermal spraying, electric arc and TIG welding. *Materials Today – Proceedings*. 50(5), 1599-1605. DOI: 10.1016/j.matpr.2021.09.122.

[10] Jia, R., Liu, S., Luo, Z., Ning, J., Wang, H., Luo, T., Zhu, Y., Yuan, X. & Wang, Z. (2020). Microstructure and wear resistance of WC and high chromium cast iron hardfacing layers. *Coatings.* 10(9), 852, 1-9. DOI: 10.3390/coatings10090852.

[11] Winczek, J., Gucwa, M., Mician, M., Konar, R. & Parzych, S. (2019). The evaluation of the wear mechanism of high-carbon hardfacing layers. *Archives of Metallurgy and Materials.* 64(3), 1111-1115. DOI: 10.24425/amm.2019.129502.

[12] Vargova, M., Tavodova, M., Monkova, K. & Dzupon, M. (2022). Research of resistance of selected materials to abrasive wear to increase the ploughshare lifetime. *Metals.* 12(6), 940, 1-16. DOI: 10.3390/met12060940.

[13] Gucwa, M., Winczek, J., Beczkowski, R. & Dosipal, M. (2016). Structure and properties of coatings made with self shielded cored wire. *Archives of Foundry Engineering.* 16(3), 39-42. DOI: 10.1515/afe-2016-0046.

[14] Jhavar, S., Paul, C.P. & Jain, N.K. (2013). Causes of failure and repairing options for dies and molds: A review. *Engineering Failure Analysis.* 34, 519-535. DOI: 10.1016/j.engfailanal.2013.09.006.

[15] Kasinska, J., Skrzypczyk, A. & Kalandyk, B. (2018). Surfacing 24Cr-5Ni-2.5Mo Duplex steel castings by TIG. *Archives of Foundry Engineering.* 18(2), 15-20. DOI: 10.24425/122495.

[16] Lyczkowska, K. & Adamiec, J. (2017). Repair of precision castings made of the inconel 713C alloy. *Archives of Foundry Engineering.* 17(3), 210-216. DOI: 10.1515/afe-2017-0117.

[17] Wang, X., Han, F., Liu, X., Qu, S. & Zou, Z. (2008). Microstructure and wear properties of the Fe–Ti–V–Mo–C hardfacing alloy. *Wear.* 2008, 265(5-6), 583-589. DOI: 10.1016/j.wear.2007.12.001.

[18] Sutka, J., Konar, R., Moravec, J. & Petricko, L. (2021). Arc welding renovation of permanent steel molds. *Archives of Foundry Engineering.* 21(2), 35-40. DOI: 10.24425/ afe.2021.136095.